BioTechnologia vol. 104 (3) • pp. 275–287 • 2023
Journal of Biotechnology, Computational Biology and Bionanotechnology RESEARCH PAPERS
https://doi.org/10.5114/bta.2023.130730

Formation, characterization, and analysis of curcumin nanoformulation for evaluating its *in vitro* cytotoxicity

NILAM PARMAR [1]*, ABDULKHALIK MANSURI [2], KRUPALI TRIVEDI [3], KHAIRAH ANSARI [3], PRIYESH KUMAR [3], MOHAMMED AZIM BAGBAN [4], DEVENDRASINH JHALA [3], ALPESH PATEL [5], SHIVA SHANKARAN CHETTIAR [5]

[1] Department of Life Sciences, School of Sciences, Gujarat University, Ahmedabad, India

[2] Department of Biological and Life Sciences, School of Arts and Sciences, Ahmedabad University, Ahmedabad, India

[3] Cell and Molecular Biology Laboratory, Department of Zoology, School of Sciences, Gujarat University, Ahmedabad, India

[4] Department of Microbiology, C.U. Shah Institute of Science, Gujarat University, Ahmedabad, Gujarat, India

[5] Genexplore Diagnostics and Research Centre Pvt. Ltd., Ahmedabad, Gujarat, India

Received: 8 July 2022; revised: 5 March 2023; accepted: 18 May 2023

Abstract

Nanotechnology holds significance in all fields of research, and the formation and surface alterations of nanomaterials are particularly important in this discipline. Nanoformulations synthesized with bioactive plant components play a crucial role in the improvement of several therapeutics and diagnostics. In the present study, we reported the synthesis of a curcumin nanoformulation (CN) by using curcumin and D-α-tocopheryl polyethylene glycol 1000 succinate (TPGS). The synthesized CN was characterized using dynamic light scattering, UV-Visible spectrophotometry, Fourier-transform infrared spectroscopy, field-emission scanning electron microscopy, and X-ray diffraction. Furthermore, it was evaluated for solubility, drug loading, encapsulation efficiency, stability, *in vitro* release, and anticancer potentials. The role of TPGS in the synthesis of CN was validated. The synthesized CN exhibited a size of 6.2 ± 1.9 nm, needle-shaped morphology, a polydispersity index of 0.164, and zeta potential of −10.1 ± 3.21 mV, as determined by characterization techniques. Its water solubility was 2.5×10^4 times higher than that of pure curcumin. The encapsulation efficiency and curcumin loading efficiency of the synthesized CN were found to be 80 and 10%, respectively, with storage stability exceeding 30 days. Moreover, the synthesized CN demonstrated significant *in vitro* anticancer activity against the colorectal cancer cell line HCT-116, with an IC50 value of 12.74 ± 0.54 μM at 24 h.

Key words: anticancer, curcumin nanoformulation, D-α-tocopheryl polyethylene glycol 1000 succinate, solubility, stability

Introduction

Nanoparticle-based drug delivery systems obtained significant consideration in the area of nanotechnology due to their unique characteristics, such as a large surface area, high reactivity, and improved solubility. These properties enable the efficient delivery of therapeutic agents to specific target sites, minimizing systemic toxicity and enhancing therapeutic efficacy. In particular, nanomaterials synthesized using bioactive components derived from plants have emerged as a natural and eco-friendly approach (Dillard and German, 2000). Various bioactive plant components, including curcumin (Hettiarachchi et al., 2021), quercetin (Parhi et al., 2020), kaempferol (Kazmi et al., 2021), rutin (Zhang and Han, 2018), berberine (Javed Iqbal et al., 2021), and others, have been employed for the synthesis of nanomaterials.

* Corresponding author: Department of Life Sciences, School of Sciences, Gujarat University, Ahmedabad-380009, India; e-mail: nilamparmar538@gmail.com

However, curcumin nanoformulations have received the most extensive research and evaluation for various pharmaceutical applications.

One of the major reasons for extensive research on curcumin nanoformulations is the extremely low solubility and bioavailability of curcumin in its free form. Curcumin is a plant-based polyphenol compound derived from the rhizomes of Curcuma longa, commonly known as turmeric (Hewlings and Kalman, 2017). It possesses numerous pharmaceutical potentials, including anti-inflammatory (Peng et al., 2021), antioxidant (He et al., 2015), anticancer (Tomeh et al., 2019; Abd Wahab et al., 2020; Mirzaei et al., 2021; Danduga et al., 2022; Namwan et al., 2022), antimicrobial (Adamczak et al., 2020), and antimutagenic (Khan and Ahmad, 2020) effects. However, its therapeutic potential is hindered by its hydrophobic nature, which results in low systemic exposure and rapid clearance from the body.

To overcome these limitations associated with hydrophobic drugs, D-α-tocopheryl polyethylene glycol 1000 succinate (TPGS) is commonly employed for solubilization, emulsification, permeation, and stabilization in drug development (Zou and Gu, 2013; Gaonkar et al., 2017; Tan et al., 2017; Yang et al., 2018). TPGS has been recognized by the US Food and Drug Administration as a pharmacologically acceptable supplement for oral, parenteral, topical, nasal, and rectal/vaginal administration (Monteiro-Riviere et al., 2005; Van Hamme et al., 2006).

Earlier studies have demonstrated the safety of TPGS-based nanoparticles for oral administration and their extensive use in delivering curcumin to enhance its aqueous solubility (Vijayakumar et al., 2016; Meng et al., 2017). TPGS-Curcumin micelles, with a particle size of 12 nm, have been utilized to encapsulate curcumin, thereby improving its solubility and bioavailability, and enabling oral administration (Li et al., 2019). In this present study, we synthesized a curcumin nanoformulation (CN) with certain modifications, resulting in smaller formulations compared to the TPGS-Curcumin micelles synthesized by Li et al. (2019).

Chen et al. (2022) successfully synthesized curcumin-loaded nanoparticles using a blend of PLGA and TPGS, which exhibited significant anticancer activity against hepatocellular carcinoma cells. Another study conducted by Nguyen et al. (2021) demonstrated the antitumor activity of curcumin nanoparticles based on Polylactic acid-TPGS. In a study by Song et al. (2016), a solid dispersion nanoformulation of curcumin-TPGS was synthesized to improve the aqueous solubility, dispersion ratio, bioavailability, and cellular absorption of curcumin.

This study aimed to synthesize a highly efficient CN with a smaller particle size, improved aqueous solubility, and enhanced physical stability compared to pure curcumin. The synthesized CN was subjected to comprehensive physicochemical characterization, and its *in vitro* anticancer activity was evaluated using colorectal cancer cells (HCT-116). The study highlights the potential of nanoformulations to enhance the dispersion of hydrophobic drugs like curcumin in water. Furthermore, it underscores the promising anticancer properties of curcumin, suggesting its potential application as a therapeutic agent in future anticancer treatments.

Materials and methods

Materials

Curcumin, TPGS, methanol, chloroform, and 0.1 μm filters were obtained from Sigma-Aldrich (Merck KGaA, Darmstadt, Germany), while Nanopure water was provided by Ahmedabad University. Chemicals required for animal cell cultures, including Roswell Park Memorial Institute Medium (RPMI 1640), fetal bovine serum (FBS), trypsin-EDTA, phosphate buffer saline (PBS), dimethyl sulfoxide (DMSO), and 3-(4,5-Dimethylthiazol-2-yl)-2,5-Diphenyltetrazolium Bromide (MTT), were procured from Himedia, India. The human colorectal cell line HCT-116 was obtained from NCCS, Pune, India. All materials utilized in the study were of pharmaceutical grade.

Synthesis of curcumin nanoformulation

The synthesis of CN was performed using the thin-film rehydration method, as described by Li et al. (2019), with slight modifications. In the initial stage of the synthesis, a 0.01% methanolic solution of curcumin was slowly added dropwise to a 0.1% TPGS solution (prepared in chloroform) at a stirring speed of 600–700 rpm and a temperature of 37 °C using a magnetic stirrer (model: 10 MLH plus, REMI, Mumbai, India). The solvents were then evaporated, leaving behind a yellow film. Autoclaved Mili-Q water was used to resuspend the film and the resulting solution was centrifuged at 19 090 × g for 25 min at 4 °C using a refrigerated centrifuge (model: 5430R, Eppendorf, Hamburg, Germany). The upper translucent layer was separated, and to eliminate any free curcumin particles, the solution was filtered using

a 0.1 μm filter. The final product obtained after filtration was considered the CN.

Lyophilization of synthesized CN

The synthesized CN exhibited stickiness, necessitating the use of a suitable cryoprotectant to reduce this stickiness during the lyophilization process. A 10% w/v mannitol solution was prepared, and one part of this solution was mixed with three parts of the synthesized product, using a 1 : 3 ratio. The mixture was then frozen at −80 °C overnight and subsequently subjected to drying using a Vacuum Freeze Dryer (model: FD-10-MR, LABFREEZ, Beijing, China) at −40 °C and 0.4 bar pressure for 24 h. The resulting lyophilized powder was stored at 25 °C for further experimentation.

Solubility in water

Ten milligram of pure curcumin powder and synthesized CN were individually redispersed by dissolving them in 1 ml of nanopure water using separate transparent glass vials. This was achieved through gentle shaking and stirring. The visual observation method was employed to monitor the formation of aggregates or precipitates.

Particle size measurement

The particle size analysis of the synthesized CN was conducted using dynamic light scattering (DLS) with the Zetasizer Nano-ZS instrument (Malvern Panalytical, Malvern, United Kingdom). To perform the analysis, 1 mg/ml of synthesized CN was dissolved in nanopure water. Then, 10 μl of this suspension was diluted to a final volume of 1 ml for the analysis. The samples were prepared in triplicate for accurate measurements.

Zeta potential and polydispersity index

The zeta potential (ZP) and polydispersity index (PDI) of the CN solution were determined using the Zetasizer Nano ZS90 instrument (Malvern Panalytical, Malvern, United Kingdom) at a temperature of 25 °C. To analyze the ZP, 1 ml of the CN solution was evaluated to determine the electrical charge of the solution.

Percentage of curcumin loading and encapsulation efficiency

To determine the curcumin loading and encapsulation efficiency (EE) of the synthesized CN, a range of curcumin concentrations (1–15 mg) were dissolved in methanol and added to 100 mg of TPGS solution, prepared in 5 ml of chloroform. The mixture was stirred at 600–700 rpm and maintained at 37 °C until the solvent evaporated. The resulting dried film, containing the entire CN, was then solubilized in nanopure water and filtered using a 0.1 μm syringe filter to separate any non-encapsulated CN present. The filtrate was analyzed for further examination.

The optical density of the filtrate was measured using a spectrophotometer at 425 nm, allowing for the estimation of the quantity of free curcumin content in the filtrate. The curcumin loading and EE of the synthesized CN were quantified using the following equation (Zweers et al., 2003; Bisht et al., 2007):

$$\text{Weight of encapsulated curcumin} = \text{Weight of total curcumin} - \text{Weight of filtrate curcumin} \quad (1)$$

$$\%\ \text{Curcumin loading} = \frac{\text{Weight of encapsulated curcumin}}{\text{Weight of total CN}} \times 100 \quad (2)$$

$$\%\ \text{Encapsulation of curcumin} = \frac{\text{Weight of encapsulated curcumin}}{\text{Weight of total curcumin}} \times 100 \quad (3)$$

Stability study

The synthesized CN was stored at a temperature of 4 °C in a dark amber bottle for 8 months. At specific intervals of 5, 10, 15, 30, 60, 120, and 240 days, samples were withdrawn from the stored CN for particle size analysis. The stored CN sample was dissolved in nanopure water through manual shaking, without the need for additional sonication. The presence of curcumin particle precipitation indicates the instability of the synthesized CN, while a clear solution confirms its stability (Gou et al., 2011). The particle size of the synthesized CN was analyzed using the DLS method at various time intervals to assess any changes over time.

Field-emission scanning electron microscopy

The structure of the synthesized CN was examined using a field-emission scanning electron microscope (JSM7600F, Jeol, Tokyo, Japan). To prepare the sample, the lyophilized CN was mounted onto a copper-coated sample stub. The sample was then dried at room temperature and visualized under the FE-SEM at an acceleration voltage of 5.0 kV.

UV-visible spectroscopy

The optical property of pure curcumin and synthesized CN were analyzed by taking the absorption spectra between 200 and 800 nm and measuring maximum absorbance using a UV-visible spectrophotometer LMSP-UV1900 (Labman Scientific Instruments, Chennai, India).

Fourier transform infrared spectroscopy

Synthesized CN was characterized by the occurrence of a functional group using FTIR (Perkin-Elmer FTIR-1600, USA). Spectra were taken between 500 and 4000/cm.

X-Ray diffraction

The X-ray diffraction (XRD) spectrum of the synthesized CN was obtained using a SmartLab SE Multipurpose X-ray diffractometer (Rigaku, Tokyo, Japan) and analyzed using X'Pert high source software. This analysis aimed to analyze the crystalline structure of both curcumin and the synthesized CN.

To perform the XRD analysis, samples were placed on the sample holding area of a slide and inserted into the XRD instrument. The XRD patterns of the samples were collected at a temperature of 25 °C using a Cu Kα X-ray radiation source. The scanning was conducted over a 2θ range from 10 to 70° with a step size of 0.02° and a scanning speed of 6.00°/min.

Furthermore, the average crystal size (d) of the CN was calculated using the Scherrer equation (Scherrer, 1918).

$$d\,[\mathrm{nm}] = \frac{K\lambda}{\beta \cos\theta} \tag{4}$$

where λ is the wavelength of the X-ray, β is the full width at half maximum, and θ is Bragg's angle of reflection.

In vitro release assay

For this assessment, 100 mg of lyophilized CN was dissolved in 10 ml of normal saline, and this solution was evenly distributed into 10 vials. The vials were then incubated at a temperature of 37 °C for a maximum time of 48 h.

After the incubation period, the mixture was centrifuged at 19 090 × g for 3 min to separate the unencapsulated curcumin that remained in the nanoformulation. The free curcumin was obtained as a pellet and solubilized in methanol.

The absorbance of the solubilized curcumin was measured at a wavelength of 425 nm. The percentage release of curcumin was calculated using the provided formula.

$$\%\,\text{Release of curcumin} = \frac{\text{Weight of released curcumin}}{\text{Weight of total curcumin}} \times 100 \tag{5}$$

In vitro anticancer activity of the synthesized CN

HCT-116 human colorectal cells were cultured in complete RPMI 1640 media supplemented with 10% FBS, penicillin (100 U/ml), and streptomycin (100 μg/ml). The cell culture was maintained at a temperature of 37 °C with 5% CO_2 in a humidified environment.

Cytotoxicity analysis was conducted using the MTT assay, as described by Mosmann in 1983. Briefly, HCT-116 cells were seeded in a 96-well plate at a density of 10^4 cells/well and incubated overnight for cell attachment. After that, the cells were treated with various concentrations (ranging from 1.25 to 100 μM) of the synthesized CN, curcumin, TPGS, and the corresponding amount of cisplatin for a duration of 24 h.

Stock solutions of curcumin and cisplatin were prepared in DMSO at a concentration of 1% (v/v) and then diluted with RPMI 1640 media. Subsequently, 20 μl of MTT solution (5 mg/ml) was added to each well and incubated for 3 h. After incubation, 100 μl of DMSO was added to dissolve the formazan crystals formed. The optical density of each well was measured at 570 nm using a Microplate Spectrophotometer (Epoch BioTeck Instruments, Winooski, Vermont, United States). All experimental groups were analyzed in triplicate.

Statistical analysis

The obtained data were expressed as mean ± standard error based on triplicate experiments. To assess the significance of the results, the mean values of the treated groups were compared to the control group. Statistical analysis was performed using the ordinary one-way ANOVA test, utilizing GraphPad Prism 8.4.3 version. A P-value <0.05 was considered statistically significant.

Results and discussion

Solubility test of CN

In this study, we successfully synthesized a water-soluble CN using the thin-film hydration method. The water solubility of pure curcumin was reported to be

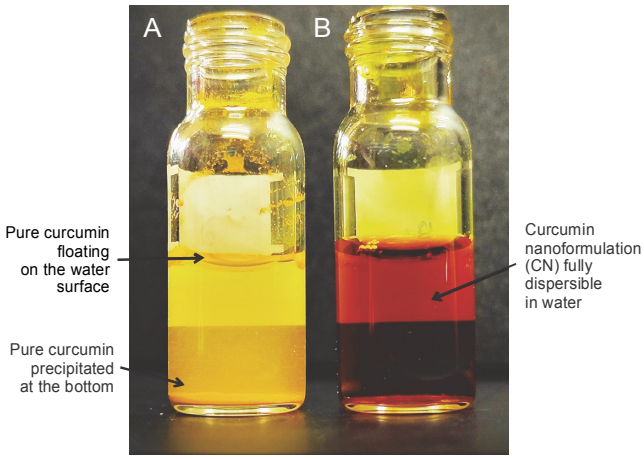

Fig. 1. Solubility test of curcumin (A) and curcumin nanoformulation (B)

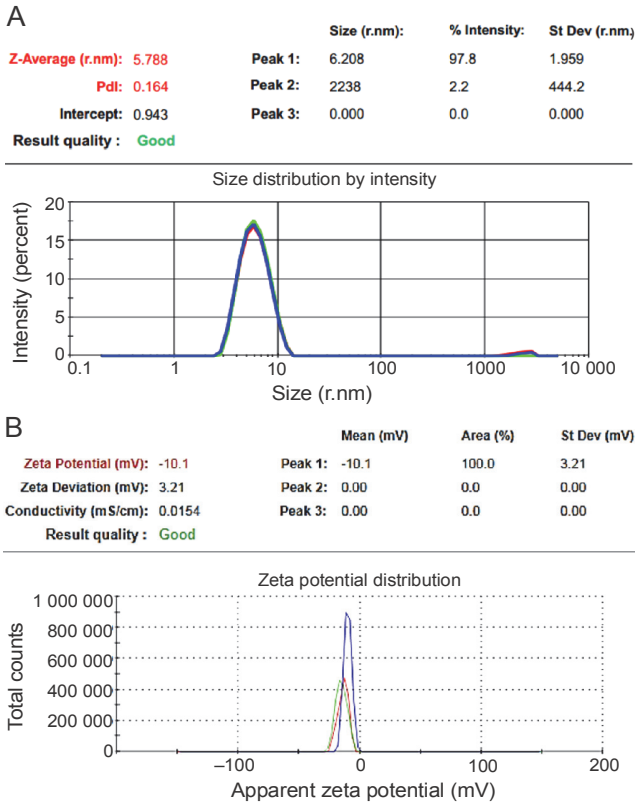

Fig. 2. Particle size (A) and zeta potential (B) analysis of curcumin nanoformulation

0.0004 mg/ml (Yallapu et al., 2012), as evidenced by the presence of insoluble microflakes on the surface of nanopure water and at the bottom of the glass vial (Fig. 1A). However, the synthesized CN was finely dispersed in water (Fig. 1B) due to encapsulation in TPGS and the formation of a nanoformulation. The solubility of curcumin was significantly increased up to 10 mg/ml in the synthesized CN compared to pure curcumin, corresponding to a 2.5×10^4-fold enhancement in solubility. It was observed that the water solubility of the synthesized CN was ~13 times higher than TPGS-stabilized curcumin nanoparticles (Rachmawati et al., 2016). This indicated that the water solubility of the synthesized CN was superior to TPGS-stabilized curcumin nanoparticles. Consequently, it can be inferred that curcumin becomes highly dispersible and soluble in an aqueous medium after encapsulation in the nanoformulation, leading to an increase in bioavailability (Bosselmann and Williams, 2012). Thus, the synthesized CN effectively addressed the major limitation of curcumin, which is poor water solubility. Additionally, the increased water solubility of curcumin after nanoformulation reduces the requirement for solvents and lowers the risk of solvent toxicity without the need for large amounts of solvents.

Particle size, PDI, and ZP

To confirm the synthesis of CN and analyze its particle size, PDI values, and ZP, the dynamic light scattering method was employed. The results revealed that the average particle size of the synthesized CN was 6.2 ± ± 1.9 nm with a PDI value of 0.164 (Fig. 2A). The ZP of the synthesized CN was −10.1 ± 3.21 mV (Fig. 2B). The particle size of the synthesized CN was approximately 50% smaller than previously synthesized TPGS-curcumin nanoparticles (12.3 ± 0.1 nm) (Montes-Burgos et al., 2009). The PDI value of the synthesized CN fell within the range of 0.0 to 1.0, indicating a homogeneous population of the nanoformulation (Chen et al., 2011; Badran, 2014; Putri et al., 2017). Additionally, the ZP value of the synthesized CN was comparable to the ZP values of −12.50 and −13 mV reported in studies by Rachmawati et al. (2013) and Luiz et al. (2022), respectively. This similarity can be attributed to the presence of ionizing groups in the structure of TPGS. Previous studies have shown that curcumin-TPGS mixed micelles, synthesized using an improved film dispersion technique, had a particle size of 65.54 ± 2.57 nm, a PDI value of 0.114 ± 0.027, and an average ZP value of −14.90 ± 2.50 mV, demonstrating increased stability in dispersion (Ji et al., 2018). It has been reported that a ZP value of approximately −15 mV exhibits greater accumulation at the tumor site and extended retention time in the blood compared to nanoparticles with more

negative or positive charges (Faraji and Wipf, 2009). However, it should be noted that the stabilization of particles by electrostatic repulsion is typically effective only when the ZP is above ±30 mV, raising questions about the stabilization of the synthesized CN solely based on the ZP (Mengual et al., 1999; Gao et al., 2010). Previous studies have highlighted that the size of nanoparticles affects tissue distribution and membrane permeability of the drug of interest (Islam et al., 2017). Due to their large surface area, high drug loading capacity, controlled drug release, biocompatibility, and smaller particle size, nanoformulations have demonstrated a significant impact on the management and prognosis of various diseases for *in vivo* applications (Soo Choi et al., 2007). Therefore, the findings suggest that the smaller particle size, significant PDI value, and ZP of the synthesized CN make it suitable for further *in vivo* applications.

Drug loading percentage and encapsulation efficiency percentage

The percentage of curcumin loading at different curcumin amounts (2–14 mg) in 100 mg of TPGS is presented in Fig. 3A. The study demonstrated that the synthesized CN achieved a loading capacity of 10% for curcumin (Fig. 3A) with an EE of 80% (Fig. 3B), which was higher than other curcumin-loaded TPGS nanoformulations reported in the literature. For example, a curcumin-loaded TPGS nanoformulation achieved 8.17% loading of curcumin and 85% EE (He et al., 2010). Curcumin loaded in Pluronic P123 micelles exhibited only 4% loading capacity and 46% EE (Ganguly et al., 2017), while curcumin loaded in casein micelles showed 4% loading capacity and 81% EE (Pan et al., 2014). Another study reported 3.24% loading and 83% encapsulation of crizotinib using TPGS (Wang et al., 2022). TPGS has been shown to enhance EE and the amount of released curcumin at the targeted site during targeted cancer therapy (Sun et al., 2021). High drug-loading capacity is advantageous as it reduces the amount of nanoformulation required to achieve therapeutic efficacy, minimizing drug overdose and production costs associated with anticancer drug delivery nanoformulations (Shen et al., 2017). Therefore, the synthesized CN shows promise as a potential agent for the delivery of curcumin in anticancer therapy.

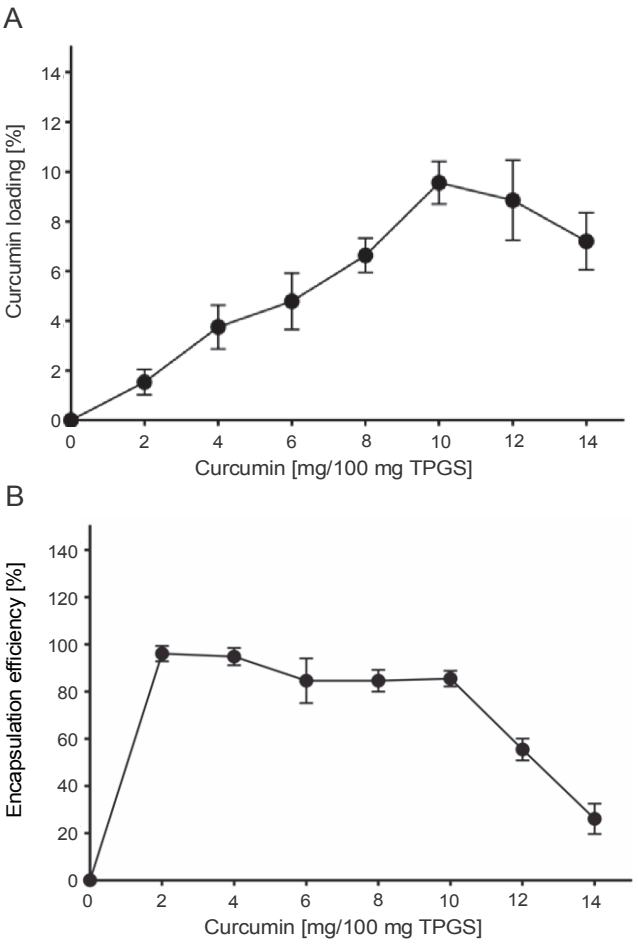

Fig. 3. Percentage of drug loading (A) and encapsulation efficiency (B) of curcumin nanoformulation

Stability study

The stability of the synthesized CN was evaluated by measuring the particle size after storage at room temperature for up to 2 months. Figure 4A shows that the synthesized CN particles maintained a uniform size without any aggregation during the 2-month storage period. In comparison, curcumin-encapsulated nanoparticles synthesized by Dai et al. (2019) exhibited a particle size of approximately 103 nm and storage stability for only 1 month at room temperature. After 2 months of storage, we observed a gradual increase in the particle size of the synthesized CN. According to Stoke's law, the particle diameter is proportional to the sedimentation rate (McClements, 2015). Consequently, smaller particles exhibit slower movement and are less prone to accumulation. Based on this understanding, we hypo-

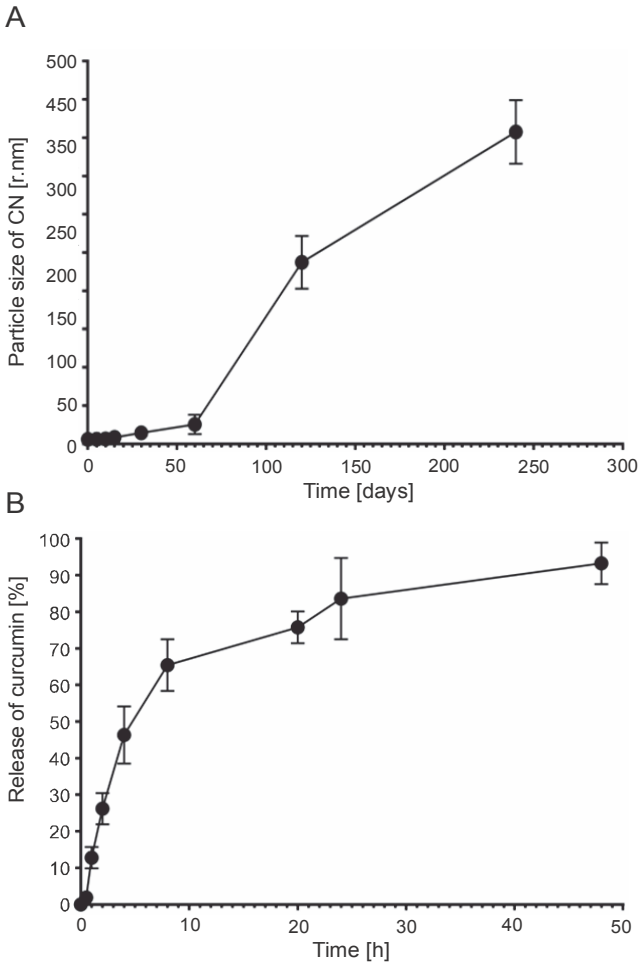

Fig. 4. The storage stability analysis of curcumin nanoformulation (A) and *in vitro* percentage release profile of curcumin (B) from curcumin nanoformulation up to 48 h

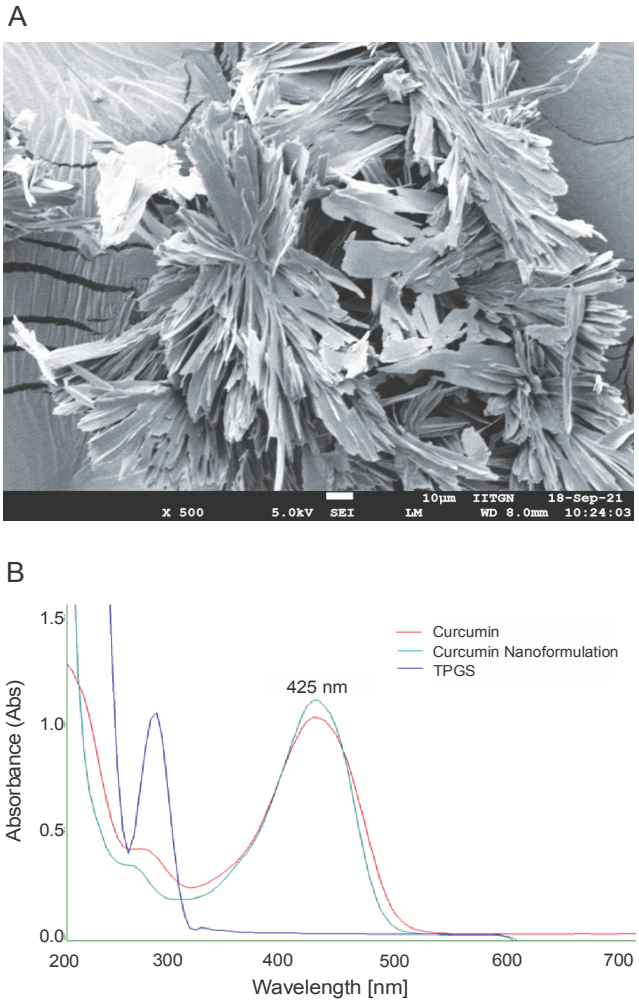

Fig. 5. Morphological analysis of curcumin nanoformulation by field-emission scanning electron microscopy (A) and UV-Visible spectrophotometric analysis of curcumin and curcumin nanoformulation (B)

thesize that the smaller particle size of the synthesized CN contributes to its long-term stability of up to 2 months without aggregation.

Field-emission scanning electron microscopy

The FE-SEM analysis of the synthesized CN revealed needle-shaped surface crystal structures, as depicted in Fig. 5A. This surface morphology is consistent with previous studies on curcumin nanocrystals obtained through the precipitation method (He et al., 2010; Rajasekar and Devasena, 2015; Ndong Ntoutoume et al., 2016). According to Junghanns and Müller (2008), nanocrystals are colloidal systems characterized by highly stable nanosized cores surrounded by surfactant molecules. Nanocrystals offer several advantages, including improved stability, enhanced drug loading capacity, cost-effectiveness, and improved dissolution rates for hydrophobic drugs (Wang et al., 2013; Danhier et al., 2014). The needle-shaped structure observed in the synthesized CN can be attributed to its increased water solubility (Sharifi et al., 2020). These advantages have contributed to the growing popularity of nanocrystals as an innovative delivery system for poorly water-soluble phytochemicals such as curcumin.

UV-Visible spectroscopy

The UV-Visible spectral analysis demonstrated that the synthesized CN exhibited a similar absorption peak at a wavelength of 425 nm, comparable to pure curcumin (Fig. 5B). This finding is consistent with the absorption spectra of curcumin-loaded nanoparticles synthesized by Wang et al. (2018a), which also exhibited a prominent

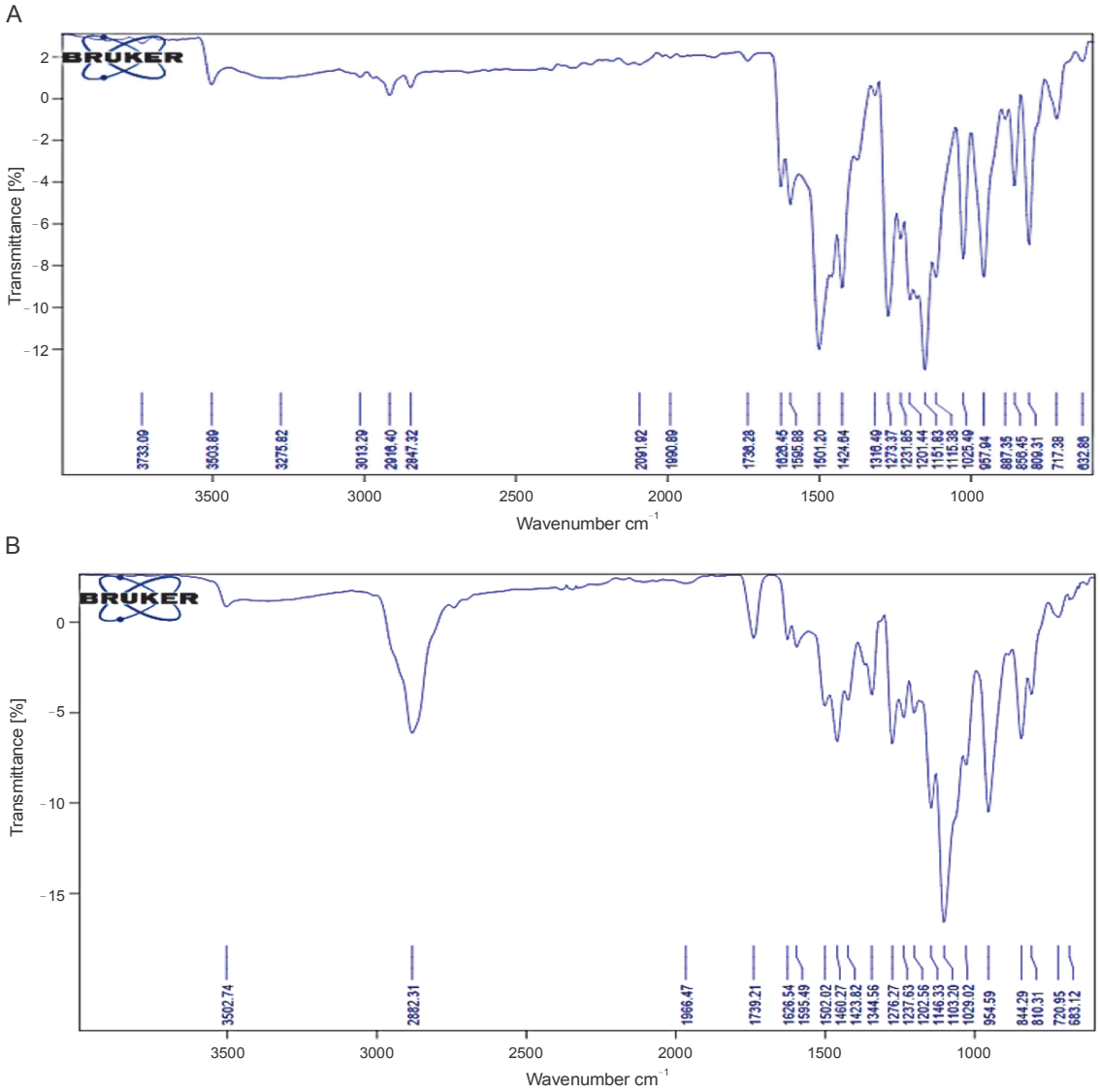

Fig. 6. Fourier transform infrared (FTIR) spectra of curcumin (A) and curcumin nanoformulation (B)

absorption peak at 425 nm. This similarity in absorption maxima indicates that curcumin was successfully entrapped during the synthesis of the nanoformulation. It suggests that the chemical composition of curcumin remained intact throughout the synthesis process, with no significant structural changes occurring in the curcumin molecule. Moreover, this observation implies that curcumin retains its biochemical properties and pharmacological potential even after being incorporated into the CN formulation.

Fourier transform infrared spectroscopy

The FTIR spectra (Fig. 6B) of the synthesized CN exhibited characteristic peaks corresponding to the functional groups present in curcumin, which were also observed in the FTIR spectrum of pure curcumin (Fig. 6A). These characteristic peaks include vibrations at 1025.49 and 1029.02/cm (C–O–C stretching), 1273.37 and 1276.27/cm (aromatic C–O stretching), 1424.64 and 1423.82/cm (olefinic C–H bending), 1626.45 and 1626.54/cm (C=C vibrations), 2847.32 and 2882.31/cm (C–H methyl ring), and 3503.89 and 3502.74/cm (phenolic O–H stretching). These findings are consistent with previous studies by Rompicharla et al. (2017), Wang et al. (2018b), and Hettiarachchi et al. (2021) which also reported the presence of these functional groups in curcumin. The presence of these characteristic functional groups in the synthesized CN confirms that there were

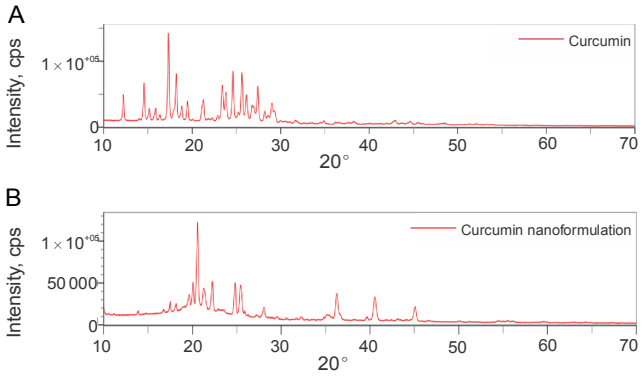

Fig. 7. X-ray diffraction (XRD) spectra of curcumin (A) and curcumin nanoformulation (B)

no significant structural alterations in the curcumin molecule during the synthesis process. Therefore, the synthesized CN can be considered a suitable drug carrier or nanoformulation for *in vitro* and *in vivo* experiments, as it protects the curcumin molecule from disintegration and preserves its biochemical properties.

X-ray diffraction

The XRD analysis was conducted to examine the crystalline structure of pure curcumin and the synthesized CN. In both cases, the XRD patterns exhibited high peak intensities in the range of 10–30 positions at a diffraction angle of 2θ, indicating the crystalline nature of curcumin (Fig. 7A) and curcumin present in the synthesized CN (Fig. 7B). The similarity in peak intensities between curcumin and curcumin in the synthesized CN suggests that the curcumin molecule was preserved and not degraded during the production of the nanoformulation (Peng et al., 2018; Taghavifar et al., 2022).

Additionally, the average crystallite domain size of the synthesized CN was calculated to be 7.87 nm using the relevant formula. This value is in close proximity to the particle size measured by DLS analysis, indicating that the synthesis protocol resulted in the production of significantly smaller nanoformulations without altering the structural characteristics of curcumin.

In vitro release profile of the synthesized CN

The *in vitro* release profile of curcumin from the synthesized CN was evaluated at 37°C using a saline solution with a pH of 7.4. The release profile, as shown in Fig. 4B, demonstrated that the synthesized CN exhibited an initial burst release of approximately 25% of

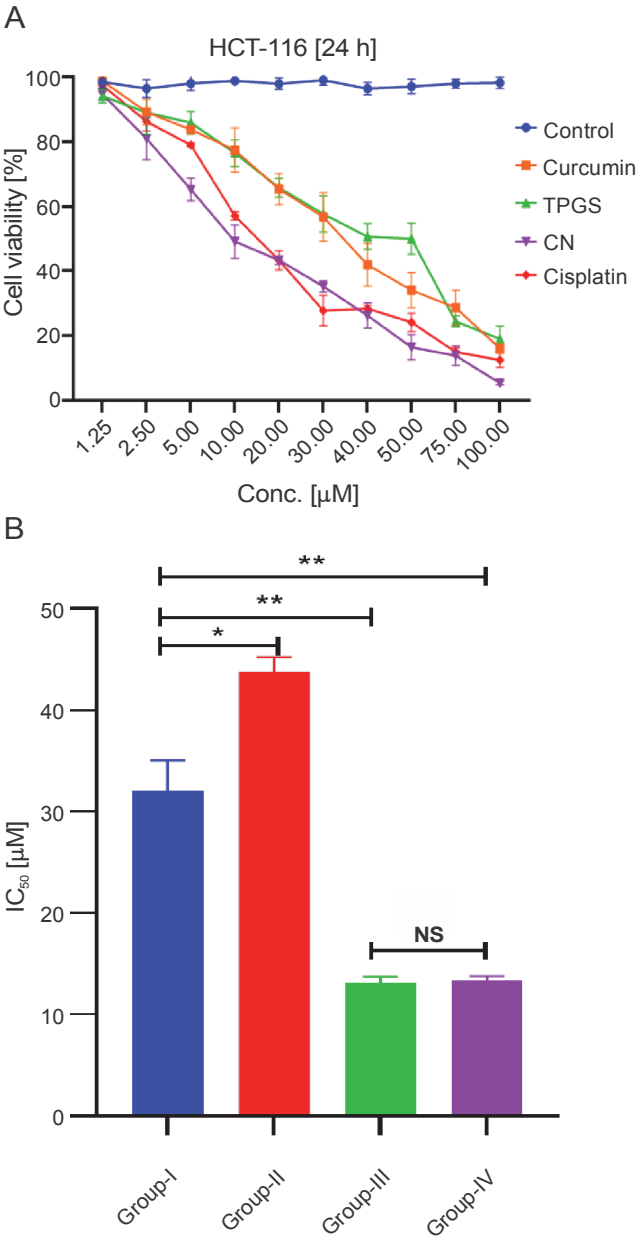

Fig. 8. The % cell viability was determined by MTT assay after the treatment of various concentrations (1.25–100 µM), curcumin (Group I), TPGS (Group II), CN (Group III), and cisplatin (Group IV) on HCT-116 cells at 24 h (A); IC_{50} values were plotted with mean ± SE; $^{*}P < 0.001$, $^{**}P < 0.0001$ when Groups II, III, and IV were compared with Group I; NS – non significant when Group III was compared with Group IV (B)

curcumin within the first 4 h. This initial burst release may be attributed to the curcumin molecules that were adsorbed on the surface of the nanoformulation.

Following the initial burst release, the release profile demonstrated a sustained and stable release of curcumin for up to 10 h. After 24 h, the cumulative release of curcumin reached approximately 80%. This release profile

Table 1. The IC_{50} values of treated groups on the HCT-116 cell line at 24 h

Groups	Treatment	IC_{50} [μM] (mean ± SE)	*P*-value
I	pure curcumin	32.335 ± 3.525	–
II	TPGS	41.984 ± 2.620	< 0.001 (when compared with Group I)
III	synthesized CN	12.745 ± 0.542	< 0.0001 (when compared with Group I)
IV	cisplatin	13.328 ± 0.351	< 0.0001 (when compared with Group I); NS (when compared with Group IV)

NS – non significant

indicates that the synthesized CN has a higher curcumin release compared to the study that reported only 50% curcumin release after 24 h (Rachmawati et al., 2016).

Anticancer activity of the synthesized CN

The anticancer activity of the synthesized CN was evaluated using the MTT assay, and the results, as shown in Fig. 8A, demonstrated that the synthesized CN significantly inhibited the growth of HCT-116 cells compared to the control (untreated) and pure curcumin. The IC_{50} value of the synthesized CN after 24 h of treatment was found to be 12.74 ± 0.54 and 32.33 ± 3.52 μM, respectively (Table 1). While the IC_{50} value of TPGS and cisplatin (positive control) for 24 h were 41.984 ± 2.62 and 13.32 ± 0.35 μM, respectively.

Comparing the IC_{50} values, it was observed that the synthesized CN exhibited a significantly lower IC50 value ($P < 0.001$) compared to TPGS, whereas it was significantly higher ($P < 0.0001$) as compared to synthesized CN and cisplatin. The IC_{50} value of synthesized CN (12.74 ± 0.54 μM) was almost similar to the metal-based anticancer drug cisplatin (13.32 ± 0.35 μM) which indicated that the synthesized CN more significantly inhibited the cell growth with similar anticancer activity of cisplatin (Fig. 8B). This suggests that the combination of CN and cisplatin with their similar effects may increase the efficacy of therapeutic response and decrease the mortality cancer patients (Sandhiutami et al., 2021). The IC_{50} value of CN optimized by Wadhwa et al. (2014) was noted as 20.32 μM on the HT-29 colorectal cancer cell line which is a higher IC_{50} value than the synthesized CN on HCT-116. One of the primary goals of this study was to put a step forward in developing an effective CN as an appropriate strategy for either primary or supplementary cancer treatment.

Overall, the proven anticancer potential of the synthesized CN supports its further exploration for biomedical and pharmaceutical applications.

Conclusion

In summary, the successful synthesis of TPGS-based crystalline CN using nanotechnology has provided several advantages, including smaller particle sizes, good storage stability, and rapid dispersibility in aqueous media. These characteristics enable the effective delivery of curcumin, a hydrophobic molecule, and enhance its anticancer activity.

The curcumin loading and EE results indicate that the synthesized CN is an efficient delivery system for curcumin. This study proved that synthesized CN enhanced the anticancer activity of curcumin *in vitro*. Moreover, the results demonstrated the potential of synthesized CN as a therapeutic approach for the management of various cancers, and supplementary research is necessary to determine its clinical potential.

Acknowledgments

This study was supported by the Scheme of developing high-quality research (SHODH) from the Government of Gujarat, India (Ref. No. 201901380079). The authors are thankful to the lab facility of Ahmedabad University for the DLS analysis, Central Instrumentation Facility of IIT Gandhinagar for ZP analysis and FE-SEM analysis, and Department of Physics, Gujarat University for XRD analysis.

Conflict of interest

The authors declared that this study had no conflicts of interest.

References

Abd Wahab N.A., Lajis N.H., Abas F., Othman I., Naidu R. (2020) *Mechanism of anti-cancer activity of curcumin on androgen-dependent and androgen-independent prostate cancer.* Nutrients 12(3): 679.

Adamczak A., Ożarowski M., Karpiński T.M. (2020) *Curcumin, a natural antimicrobial agent with strain-specific activity.* Pharmaceuticals (Basel) 13(7): 153.

Badran M. (2014) *Formulation and in vitro evaluation of flufenamic acid-loaded deformable liposomes for improved skin delivery*. Dig. J. Nanomater. Biostruct. 9(1): 83–91.

Bosselmann S., Williams R.O. (2012) *Has nanotechnology led to improved therapeutic outcomes?* Drug Dev. Ind. Pharm. 38(2): 158–170.

Chen M., Liu X., Fahr A. (2011) *Skin penetration and deposition of carboxyfluorescein and temoporfin from different lipid vesicular systems: in vitro study with finite and infinite dosage application.* Int. J. Pharm. 408(1–2): 223–234.

Chen X., Li Y., Zhang Y., Li G. (2022) *Formulation, characterization and evaluation of curcumin-loaded PLGA-TPGS nanoparticles for liver cancer treatment.* Drug Des. Devel. Ther. 13(2019): 3569–3578.

Dai L., Zhou H., Wei Y., Gao Y., McClements D.J. (2019) *Curcumin encapsulation in zein-rhamnolipid composite nanoparticles using a pH-driven method.* Food Hydrocoll. 93(2019): 342–350.

Danduga R.C.S.R., Kola P.K., Matli B. (2022) *Anticancer activity of curcumin alone and in combination with piperine in Dalton lymphoma ascites bearing mice.* Indian J. Exp. Biol. 58(3): 181–189.

Danhier F., Ucakar B., Vanderhaegen M.L., Brewster M.E., Arien T., Préat V. (2014) *Nanosuspension for the delivery of a poorly soluble anti-cancer kinase inhibitor.* Eur. J. Pharm. Biopharm. 88(1): 252–260.

Dillard C.J., German J.B. (2000) *Phytochemicals: nutraceuticals and human health.* J. Sci. Food Agric. 80(12): 1744–1756.

Faraji A.H., Wipf P. (2009) *Nanoparticles in cellular drug delivery*. Bioorg. Med. Chem. 17(8): 2950–2962.

Ganguly R., Kunwar A., Kota S., Kumar S., Aswal V.K. (2018) *Micellar structural transitions and therapeutic properties in tea tree oil solubilized pluronic P123 solution*. Colloid. Surf. A: Physicochem. Engin. Aspects 537: 478–484.

Gao Y., Li Z., Sun M., Li H., Guo C., Cui J., Li A., Cao F., Xi Y., Lou H. et al. (2010) *Preparation, characterization, pharmacokinetics, and tissue distribution of curcumin nanosuspension with TPGS as stabilizer.* Drug Dev. Ind. Pharm. 36(10): 1225–1234.

Gaonkar R.H., Ganguly S., Dewanjee S., Sinha S., Gupta A., Ganguly S., Chattopadhyay D., Chatterjee Debnath M. (2017) *Garcinol loaded vitamin E TPGS emulsified PLGA nanoparticles: preparation, physicochemical characterization, in vitro and in vivo studies*. Sci. Rep. 7(1): 530.

Gou M., Men K., Shi H., Xiang M., Zhang J., Song J., Long J., Wan Y., Luo F., Zhao X. et al. (2011) *Curcumin-loaded biodegradable polymeric micelles for colon cancer therapy in vitro and in vivo*. Nanoscale 3(4): 1558–1567.

He Y., Huang Y., Cheng Y. (2010) *Structure evolution of curcumin nanoprecipitation from a micromixer*. Cryst. Growth Des. 10(3): 1021–1024.

He Y., Yue Y., Zheng X., Zhang K., Chen S., Du Z. (2015) *Curcumin, inflammation, and chronic diseases: how are they linked?* Molecules 20(5): 9183–9213.

Hettiarachchi S.S., Dunuweera S.P., Dunuweera A.N., Rajapakse R.M.G. (2021) *Synthesis of curcumin nanoparticles from raw turmeric rhizome.* ACS Omega 6(12): 8246–8252.

Hewlings S.J., Kalman D.S. (2017) *Curcumin: a review of its effects on human health.* Foods 6(10): 92.

Islam M.A., Barua S., Barua D. (2017) *A multiscale modeling study of particle size effects on the tissue penetration efficacy of drug-delivery nanoparticles*. BMC Syst Biol. 11: 113.

Javed Iqbal M., Quispe C., Javed Z., Sadia H., Qadri Q.R., Raza S., Salehi B., Cruz-Martins N., Abdulwanis Mohamed Z., Sani Jaafaru M., Abdull Razis A.F., Sharifi-Rad J. (2021) *Nanotechnology-based strategies for berberine delivery system in cancer treatment: pulling strings to keep berberine in power.* Front Mol. Biosci. 7: 624494.

Ji S., Lin X., Yu E., Dian C., Yan X., Li L., Zhang M., Zhao W., Dian L. (2018) *Curcumin-loaded mixed micelles: preparation, characterization, and in vitro antitumor activity*. J. Nanotechnol. 2018: 9103120.

Junghanns J.-U.A.H., Müller R.H. (2008) *Nanocrystal technology, drug delivery and clinical applications.* Int. J. Nanomed. 3(3): 295–310.

Kazmi I., Al-Abbasi F.A., Afzal M., Altayb H.N., Nadeem M.S., Gupta G. (2021) *Formulation and evaluation of kaempferol loaded nanoparticles against experimentally induced hepatocellular carcinoma: in vitro and in vivo studies.* Pharmaceutics 13(12): 2086.

Khan M.S., Ahmad I. (2020) *Diversity of antimutagenic phytocompounds from indian medicinal plants*. [in:] *Herbal medicine in India: indigenous knowledge, practice, innovation and its value.* Ed. Sen S., Chakraborty R. Springer-Singapore: 401–412.

Li H., Yan L., Tang E.K.Y., Zhang Z., Chen W., Liu G., Mo J. (2019) *Synthesis of TPGS/curcumin nanoparticles by thin-film hydration and evaluation of their anti-colon cancer efficacy in vitro and in vivo*. Front Pharmacol. 10: 769.

Luiz M.T., Dutra J.A.P., de Cássia Ribeiro T., Carvalho G.C., Sábio R.M., Marchetti J.M., Chorilli M. (2022) *Folic acid-modified curcumin-loaded liposomes for breast cancer therapy.* Colloids Surfac. A: Physicochem. Engin. Aspects 645: 128935.

McClements D.J. (2015) *Food emulsions: principles, practices, and techniques*. Boca Raton: CRC Press.

Meng X., Liu J., Yu X., Li J., Lu X., Shen T. (2017) *Pluronic F127 and D-α-tocopheryl polyethylene glycol succinate (TPGS) mixed micelles for targeting drug delivery across the blood brain barrier*. Sci. Rep. 7(1): 2964.

Mengual O., Meunier G., Cayré I., Puech K., Snabre P. (1999) *TURBISCAN MA 2000: multiple light scattering measurement for concentrated emulsion and suspension instability analysis*. Talanta 50(2): 445–456.

Mirzaei S., Zarrabi A., Hashemi F., Zabolian A., Saleki H., Ranjbar A., Seyed Saleh S.H., Bagherian M., Sharifzadeh S. Omid., Hushmandi K., et al. (2021) *Regulation of nuclear factor-kappaB (NF-κB) signaling pathway by non-coding RNAs in cancer: inhibiting or promoting carcinogenesis?* Cancer Lett. 509: 63–80.

Monteiro-Riviere N.A., Inman A.O., Wang Y.Y., Nemanich R.J. (2005) *Surfactant effects on carbon nanotube interactions with human keratinocytes*. Nanomedicine 1(4): 293–299.

Montes-Burgos I., Walczyk D., Hole P., Smith J., Lynch I., Dawson K. (2009) *Characterization of nanoparticle size and state prior to nanotoxicological studies.* J. Nanopart. Res. 12(1): 47–53.

Mosmann T. (1983) *Rapid colorimetric assay for cellular growth and survival: application to proliferation and cytotoxicity assays*. J. Immunol. Meth. 65(1–2): 55–63.

Namwan N., Senawong G., Phaosiri C., Kumboonma P., Somsakeesit L., Samankul A., Leerat C., Senawong T. (2022) *HDAC inhibitory and anti-cancer activities of curcumin and curcumin derivative CU17 against human lung cancer A549 cells*. Molecules 27(13): 4014.

Ndong Ntoutoume G.M.A., Granet R., Mbakidi J.P., Brégier F., Léger D.Y., Fidanzi-Dugas C., Lequart V., Joly N., Liagre B., Chaleix V., et al. (2016) *Development of curcumin–cyclodextrin/cellulose nanocrystals complexes: new anticancer drug delivery systems*. Bioorg. Med. Chem. Lett. 26(3): 941–945.

Pan K., Luo Y., Gan Y., Baek S.J., Zhong Q. (2014) *pH-driven encapsulation of curcumin in self-assembled casein nanoparticles for enhanced dispersibility and bioactivity*. Soft Matter. 10(35): 6820–6830.

Parhi B., Bharatiya D., Swain S.K. (2020) *Application of quercetin flavonoid based hybrid nanocomposites: a review.* Saudi Pharm. J. 28(12): 1719–1732.

Peng S., Li Z., Zou L., Liu W., Liu C., McClements D.J. (2018) *Improving curcumin solubility and bioavailability by encapsulation in saponin-coated curcumin nanoparticles prepared using a simple pH-driven loading method.* Food Funct. 9(3): 1829–1839.

Peng Y., Ao M., Dong B., Jiang Y., Yu L., Chen Z., Hu C., Xu R. (2021) *Anti-inflammatory effects of curcumin in the inflammatory diseases: status, limitations and countermeasures.* Drug Des. Devel. Ther. 15: 4503–4525.

Putri D.C.A., Dwiastuti R., Marchaban M., Nugroho A.K. (2017) *Optimization of mixing temperature and sonication duration in liposome preparation.* J. Pharm. Sci. Commun. 14(2): 79–85.

Rachmawati H., Shaal L.A., Müller R.H., Keck C.M. (2013) *Development of curcumin nanocrystal: physical aspects*. J. Pharm. Sci. 102(1): 204–214.

Rachmawati H., Yanda Y.L., Rahma A., Mase N. (2016) *Curcumin-loaded PLA nanoparticles: formulation and physical evaluation.* Sci. Pharma. 84(1): 191–202.

Rajasekar A., Devasena T. (2015) *Facile synthesis of curcumin nanocrystals and validation of its antioxidant activity against circulatory toxicity in Wistar rats*. J. Nanosci. Nanotechnol. 15(6): 4119–4125.

Rompicharla S.V.K., Bhatt H., Shah A., Komanduri N., Vijayasarathy D., Ghosh B., Biswas S. (2017) *Formulation optimization, characterization, and evaluation of in vitro cytotoxic potential of curcumin loaded solid lipid nanoparticles for improved anticancer activity*. Chem. Phys. Lipids. 208: 10–18.

Sandhiutami N.M.D., Arozal W., Louisa M., Rahmat D., Wuyung P.E. (2021) *Curcumin nanoparticle enhances the anticancer effect of cisplatin by inhibiting PI3K/AKT and JAK/STAT3 pathway in rat ovarian carcinoma induced by DMBA*. Front Pharmacol. 11: 603265.

Scherrer P. (1918) *Nachr Ges Wiss Goettingen*. Math. Phys. 2: 98–100.

Sharifi S., Fathi N., Memar M.Y., Hosseiniyan Khatibi S.M., Khalilov R., Negahdari R., Zununi Vahed S., Maleki Dizaj S. (2020) *Anti-microbial activity of curcumin nanoformulations: new trends and future perspectives.* Phytother. Res. 34(8): 1926–1946.

Shen S., Wu Y., Liu Y., Wu D. (2017) *High drug-loading nanomedicines: progress, current status, and prospects*. Int. J. Nanomed. 12: 4085–4109.

Song I.S., Cha J.S., Choi M.K. (2016) *Characterization, in vivo and in vitro evaluation of solid dispersion of curcumin containing D-α-tocopheryl polyethylene glycol 1000 succinate and mannitol*. Molecules 21(10): 1386.

Soo Choi H., Liu W., Misra P., Tanaka E., Zimmer J.P., Itty Ipe B., Bawendi M.G., Frangioni J.V. (2007) *Renal clearance of quantum dots*. Nat. Biotechnol. 25(10): 1165–1170.

Sun S., Du X., Fu M., Khan A.R., Ji J., Liu W., Zhai G. (2021) *Galactosamine-modified PEG-PLA/TPGS micelles for the oral delivery of curcumin*. Int. J. Pharm. 595: 120227.

Taghavifar S., Afroughi F., Saadati Keyvan M. (2022) *Curcumin nanoparticles improved diabetic wounds infected with methicillin-resistant Staphylococcus aureus sensitized with HAMLET.* Int. J. Low Extrem. Wounds. 21(2): 141–153.

Tan S., Zou C., Zhang W., Yin M., Gao X., Tang Q. (2017) *Recent developments in D-α-tocopheryl polyethylene glycol-succinate-based nanomedicine for cancer therapy*. Drug Deliv. 24(1): 1831–1842.

Nguyen D.T., Tran P.A., Ha P.T., Nguyen H.N., Nguyen X.P., Hoang, T.M.N. (2021) *Induction of apoptosis and inhibition of breast cancer cell growth and multicellular tumor spheroids by paclitaxel combined curcumin-loaded PLA-TPGS-based nanoparticles.* VNU J. Sci. Nat. Sci. Technol. 37(3): 82–91.

Van Hamme J.D., Singh A., Ward O.P. (2006) *Physiological aspects. Part 1 in a series of papers devoted to surfactants in microbiology and biotechnology*. Biotechnol. Adv. 24(6): 604–620.

Vijayakumar M.R., Vajanthri K.Y., Balavigneswaran C.K., Mahto S.K., Mishra N., Muthu M.S., Singh S. (2016) *Pharmacokinetics, biodistribution, in vitro cytotoxicity and biocompatibility of Vitamin E TPGS coated trans resveratrol liposomes*. Colloids Surf. B Biointerfac. 145: 479–491.

Wadhwa J., Asthana A., Gupta S., Shilkari Asthana G., Singh R. (2014) *Development and optimization of polymeric self-emulsifying nanocapsules for localized drug delivery: design of experiment approach.* Sci. World J. 2014: 516069.

Wang H., Wu Y., Lin X. (2022) *Crizotinib loaded polydopamine–polylactide-TPGS nanoparticles in targeted therapy for non-small cell lung cancer*. Med. Oncol. 40(1): 26.

Wang W., Chen T., Xu H., Ren B., Cheng X., Qi R., Liu H., Wang Y., Yan L., Chen S., et al. (2018a) *Curcumin-loaded solid lipid nanoparticles enhanced anticancer efficiency in breast cancer.* Molecules 23(7): 1578.

Wang Y., Luo Z., Wang Z., You M., Xie S., Peng Y., Yang H. (2018b) *Effect of curcumin-loaded nanoparticles on mitochondrial dysfunctions of breast cancer cells.* J. Nanopart. Res. 20: 283.

Wang Z., Chen B., Quan G., Li F., Wu Q., Dian L., Dong Y., Li G., Wu C. (2012) *Increasing the oral bioavailability of poorly water-soluble carbamazepine using immediate-release pellets supported on SBA-15 mesoporous silica.* Int. J. Nanomed. 7: 5807–5818.

Yallapu M.M., Jaggi M., Chauhan S.C. (2012) *Curcumin nanoformulations: a future nanomedicine for cancer.* Drug Discov. Today 17(1–2): 71–80.

Yang C., Wu T., Qi Y., Zhang Z. (2018) *Recent advances in the application of vitamin E TPGS for drug delivery.* Theranostics 8(2): 464–485.

Zhang S., Han Y. (2018) *Preparation, characterisation and antioxidant activities of rutin-loaded zein-sodium caseinate nanoparticles.* PLoS ONE 13(3): e0194951.

Zou T., Gu L. (2013) *TPGS emulsified zein nanoparticles enhanced oral bioavailability of daidzin: in vitro characteristics and in vivo performance.* Mol. Pharm. 10(5): 2062–2070.